Published in final edited form as:
J Comp Neurol. 2007 January 20; 500(3): 585–599. doi:10.1002/cne.21191.

Selective Enrichment of DJ-1 Protein in Primate Striatal Neuronal Processes: Implications for Parkinson's Disease

JAMES A. OLZMANN[1], **JILL R. BORDELON**[2], **E. CHRIS MULY**[2,3], **HOWARD D. REES**[4], **ALLAN I. LEVEY**[4], **LIAN LI**[1], and **LIH-SHEN CHIN**[1*]

Joseph L. Price

1*Department of Pharmacology, Emory University, Atlanta, Georgia, 30322*

2*Department of Psychiatry and Behavioral Sciences, Emory University, Atlanta, Georgia, 30322, USA*

3*Division of Neuroscience, Yerkes National Primate Research Center, Emory University, Atlanta, Georgia, 30322, USA*

4*Department of Neurology, Center for Neurodegenerative Disease, Emory University, Atlanta, Georgia, 30322, USA*

Abstract

Mutations in DJ-1 cause autosomal recessive, early-onset Parkinson's disease (PD). The precise function and distribution of DJ-1 in the central nervous system remain unclear. In this study, we performed a comprehensive analysis of DJ-1 expression in human, monkey, and rat brains using antibodies that recognize distinct, evolutionarily conserved epitopes of DJ-1. We found that DJ-1 displays region-specific neuronal and glial labeling in human and non-human primate brain, sharply contrasting the primarily neuronal expression pattern observed throughout rat brain. Further immunohistochemical analysis of DJ-1 expression in human and non-human primate brains showed that DJ-1 protein is expressed in neurons within the substantia nigra pars compacta and striatum, two regions critically involved in PD pathogenesis. Moreover, immunoelectron microscopic analysis revealed a selective enrichment of DJ-1 within primate striatal axons, presynaptic terminals, and dendritic spines with respect to the DJ-1 expression in prefrontal cortex. Together, these findings indicate neuronal and synaptic expression of DJ-1 in primate subcortical brain regions and suggest a physiological role for DJ-1 in the survival and/or function of nigral-striatal neurons.

Keywords

PARK7; substantia nigra; striatum; electron microscopy; primate brain; distribution

Parkinson's disease (PD) is a debilitating neurodegenerative movement disorder characterized by the relatively selective degeneration of nigral dopaminergic neurons (Lang and Lozano, 1998a; Lang and Lozano, 1998b). Recently, mutations in the gene encoding DJ-1 have been identified as the genetic defect responsible for the PARK7-associated autosomal recessive, early-onset form of familial PD (Abou-Sleiman et al., 2004; Bonifati et al., 2003). Accumulating evidence suggests that loss of DJ-1 function results in neurodegeneration, but the exact role of DJ-1 in the pathogenesis of PD is unknown (Cookson, 2005; Moore et al., 2005). Using X-ray crystallography, we and others have shown that DJ-1 is a 189 amino acid protein that adopts a helix-strand-helix dimeric structure with homology to the bacterial

*Correspondence to: Lih-Shen Chin, PhD Department of Pharmacology Emory University School of Medicine 1510 Clifton Road Atlanta, GA 30322−3090 Tel: 404−727−0361 Fax: 404−727−0365 E-mail: chinl@pharm.emory.edu.

protease PH1704 and *Escherichia coli* chaperone protein Hsp31 (Huai et al., 2003; Lee et al., 2003; Tao and Tong, 2003). Although the precise physiological function of DJ-1 remains unclear, DJ-1 has been implicated in several cellular processes including regulation of transcription, protein quality control, and oxidative stress response (Bonifati et al., 2004; Cookson, 2005; Moore et al., 2005). In addition, targeted disruption of DJ-1 gene expression in mice leads to altered dopamine D2 receptor signaling (Chen et al., 2005; Goldberg et al., 2005) and increased susceptibility to MPTP (1-methyl 4-phenyl 1,2,3,6-tetrahydropyridine)–induced neurodegeneration (Kim et al., 2005).

The distribution of DJ-1 protein is controversial and remains poorly characterized. We previously showed that DJ-1 is mainly neuronal in cortical and subcortical regions of rodent brain (Olzmann et al., 2004), and this has been confirmed by independent studies (Bader et al., 2005; Kotaria et al., 2005; Zhang et al., 2005). In contrast, DJ-1 has been reported to be present primarily in glia in human cortex (Bandopadhyay et al., 2004; Meulener et al., 2005; Miller et al., 2005; Neumann et al., 2004). These studies have prompted speculation that loss of DJ-1 function in humans may cause neuronal cell death through non-cell-autonomous processes, such as regulation of glial function (Bandopadhyay et al., 2004; Vila and Przedborski, 2004). However, a limitation of these studies is the focus on DJ-1 expression in the human cortex, and little is known regarding the subcortical distribution of DJ-1 in humans.

What is the reason(s) for the apparent differences in DJ-1 expression in human versus rat brain? Since different DJ-1 antibodies were used in the human and rat studies (Bader et al., 2005; Bandopadhyay et al., 2004; Kotaria et al., 2005; Meulener et al., 2005; Miller et al., 2005; Neumann et al., 2004; Olzmann et al., 2004; Zhang et al., 2005), the discrepancies may be due to differences in the epitopes recognized by distinct DJ-1 antibodies. Another possibility is that these observations may reflect actual differences in the distribution of DJ-1 in human and rat brains. Substantial differences between primate and rodent dopaminergic systems have been reported (Berger et al., 1991; Joel and Weiner, 2000). Knowledge of DJ-1 expression and distribution in the human brain is critical for understanding the role of DJ-1 in PD pathogenesis. However, the study of protein expression in human brain is complicated by limited tissue availability, and variable post-mortem delay and tissue preservation/fixation conditions. To overcome these problems, we analyzed the distribution of DJ-1 in non-human primate brain by immunohistochemistry and immunoelectron microscopy. As the closest phylogenetic relative of humans, non-human primates, such as macaque monkeys, have a very similar central nervous system (Berger et al., 1991; Ciliax et al., 1999; Hardman et al., 2002; Petrides and Pandya, 2002; Smiley et al., 1994). To facilitate a comprehensive and comparative analysis of DJ-1 expression across species, and to avoid inconsistencies associated with differences in epitope availability, we generated and characterized two distinct anti-DJ-1 antibodies that recognize evolutionarily conserved epitopes in primate and rodent DJ-1. Here, we report the results of immunohistochemical and ultrastructural localization studies using these antibodies to determine the distribution of DJ-1 in non-human primate brain, in addition to rat and human brains. Our findings reveal clear species differences in DJ-1 distribution in primate versus rat brain and suggest a cell-autonomous role for DJ-1 in the function and survival of primate nigral neurons.

MATERIALS AND METHODS

Antibodies

Two distinct rabbit polyclonal anti-DJ-1 antibodies, P7F and P7C, were generated against purified full-length recombinant human DJ-1 protein and a synthetic human DJ-1 carboxyl-terminal peptide (amino acids 171−189), respectively (Olzmann et al., 2004). These anti-DJ-1 antibodies recognize a single 20-kDa band in rat (Olzmann et al., 2004) and human (Choi et al., 2006). Mouse anti-DJ-1 monoclonal antibody (KAM-SA100, Stressgen) was produced

against GST-tagged full-length human DJ-1 and recognizes a single 20-kDa band in human (Miller et al., 2005). The epitope for this antibody has recently been mapped to amino acids 56−78 of human DJ-1 (Miller et al., 2005). Further characterization of these three anti-DJ-1 antibodies is described in the Results section (Fig. 1). Mouse anti-α-synuclein monoclonal antibody (#610787, BD Transduction Laboratories) was generated against amino acids 15−123 of rat synuclein-1 and recognizes a 19-kDa band in mouse, rat, and human (Manufacturers technical information). Mouse anti-tyrosine hydroxylase monoclonal antibody (MAB318, Chemicon) was produced against tyrosine hydroxylase purified from PC12 cells, recognizes a protein of approximately 60-kDa by Western blot, and reacts with human, rat, monkey, frog, and vole (Manufacturers technical information). Mouse anti-NeuN monoclonal antibody (MAB377, Chemicon) was produced against nuclei purified from mouse brain and recognizes a band of approximately 47-kDa in human, primate, rat, mouse, avian, and chicken (Manufacturers technical information). As described (Mullen et al., 1992), this antibody specifically reacts with the DNA-binding, neuronal-specific protein NeuN and has been used extensively as a marker of neurons. Mouse anti-GFAP monoclonal antibody (MAB360, Chemicon) was generated against GFAP protein purified from porcine spinal cord and recognizes a single 51-kDa band in human, bovine, porcine, rabbit, rat, and mouse (Manufacturers technical information). As described (Debus et al., 1983), GFAP is the primary component of intermediate filaments in astrocytes and this antibody has been used extensively as a marker of astrocytes. All secondary antibodies were obtained from Jackson ImmunoResearch Laboratories.

Human and Monkey Brain Samples

Human brain tissues were obtained from the Emory Center for Neurodegenerative Disease Brain Bank. Frontal cortex from five normal individuals was used for the biochemical studies (Table I). Cingulate cortex from four normal individuals and substantia nigra and striatum from one normal individual were used for the immunohistochemical studies (Table I).

Rhesus macaque brain tissues were obtained from the Yerkes National Primate Research Center at Emory University. Brain tissues from four animals were used for the biochemical studies and the immunohistochemical studies (Table I). The tissues from rhesus macaque monkeys were obtained and prepared as described previously (Bordelon et al., 2005;Muly et al., 2004a;Muly et al., 2003). The care of the animals and all anesthesia and sacrifice procedures in this study were performed according to the National Institutes for Health Guide for the Care and Use of Laboratory Animals and were approved by the Institutional Animal Care and Use Committee of Emory University. The animals were sacrificed with an overdose of pentobarbital (100 mg / kg). For the biochemical studies, brains were removed and blocks of various brain regions were immediately frozen in liquid nitrogen. For the immunohistochemical studies, the animals were perfused with a flush of Tyrode's or Ringer's solution in which 95% O_2 / 5% CO_2 was bubbled continuously. The flush was followed by 3 to 4 liters of fixative solution of 4% paraformaldehyde / 0.2% glutaraldehyde / 0−0.2% picric acid in phosphate buffer (0.1 M, pH 7.4; PB). The brain was blocked and post-fixed in 4% paraformaldehyde for 2−24 hours. Coronal, 50 μm thick vibratome sections were cut and stored frozen in 15% sucrose until immunohistochemical experiments were performed.

DJ-1 knockout mice

DJ-1 knockout (KO) mice were generated by Dr. Charles R. Gerfen at the National Institute of Mental Health. Targeted disruption of the DJ-1 gene was carried out in embryonic mouse stem cell line XE726 (BayGenomics) using a gene trap approach that inserted the beta-geo gene (a fusion of the beta-galactosidase and neomycin resistance genes) into the region between exons 6 and 7 of the murine DJ-1 gene. A breeding colony of DJ-1 knockout mice was established from breeding pairs obtained from the National Institute for Neurological Disease

and Stroke/University of California Los Angeles Repository for Parkinson's disease Mouse Models using standard mouse husbandry procedures as described previously (Chin et al., 1995). The genotype of the offspring was determined by PCR and the elimination of the DJ-1 protein was confirmed by Western blot analysis.

Western blot analysis

For Western blot analysis, human cingulate cortex, macaque prefrontal cortex, and whole brain from rat, homozygous DJ-1 KO mouse, and wild-type mouse were homogenized in 1% SDS and subjected to SDS-PAGE as described previously (Chin et al., 2002; Li et al., 2001). The proteins were transferred to nitrocellulose membranes and immunoblotted with the appropriate primary and secondary antibodies, followed by visualization using the enhanced chemiluminescence system.

Immunohistochemistry

Rat whole brains and human cingulate cortex, substantia nigra, and striatum were fixed in 4% paraformaldehyde, and processed for immunohistochemistry as described previously (Choi et al., 2004; Olzmann et al., 2004). Briefly, tissue was cryoprotected in sucrose and serial sections (50 μm) were cut on a cryostat. Sections were treated with 3% H_2O_2 to eliminate endogenous peroxidase activity and blocked with a solution containing 8% goat serum, 10 μg/ml avidin, 0.1% Triton X-100, 0.9% NaCl, and 50 mM Tris-HCl (pH 7.2). Sections were then incubated overnight at 4 °C with anti-DJ-1 (P7C or P7F, 1:8,000) followed by incubation with biotinylated secondary antibody (1:200). Bound antibodies were detected using a standard avidin-biotinylated peroxidase complex (ABC) method (Vectastain Elite ABC kit, Vector Laboratories). Sections were observed using a Leica DC500 microscope, and images were captured with a C4742−95 Hamamatsu digital camera.

Immunofluorescence confocal microscopy

Rat whole brains were fixed in 4% paraformaldehyde, processed, and double-labeling performed as described previously (Offe et al., 2006; Zhang et al., 2002). Briefly, sections were blocked and then co-incubated with anti-DJ-1 antibody (P7C, 1:8,000) and either anti-NeuN (1:50), anti-GFAP (1:1,500), or anti-tyrosine hydroxylase (1:100) antibodies overnight. Labeled DJ-1 was detected by a biotinylated-secondary antibody (1:200), followed by avid-biotinylated peroxidase complex (Vectastain Elite ABC kit, Vector Laboratories) and a tyramide-conjugated tertiary antibody (PerkinElmer). NeuN, GFAP, and tyrosine hydroxylase were detected using secondary antibodies directly conjugated to fluoroscein. After extensive washing, sections were mounted using Vectashield mounting medium (Vector Laboratories). Control samples incubated with a single primary antibody or no antibody exhibited no significant background staining. Images of immunostained sections were captured using a Zeiss LSM 510 confocal microscope using independent channels for excitation at 488 and 543.

Immunoelectron microscopy

Immunoperoxidase staining was performed using rabbit anti-DJ-1 antibodies as described previously (Muly et al., 1998). Briefly, sections were treated with a blocking solution containing 3% normal goat serum, 1% bovine serum albumin, 0.1% glycine, 0.1% lysine in 0.01 M PBS (pH 7.4) and then incubated with anti-DJ-1 antibody (P7C, 1:8000) for 36 hours at 4°C followed by incubation with biotinylated secondary antibody (1:200). Bound antibodies were detected using a standard avidin-biotinylated peroxidase complex (Vectastain Elite ABC kit) method with 3,3′-diaminobenzidine (DAB) as the chromagen. Sections were then post-fixed in osmium tetroxide, stained *en bloc* with uranyl acetate, dehydrated, and embedded in Durcupan resin (Electron Microscopy Sciences, Fort Washington, PA). Blocks of tissue from layer III of cortical area 9 and the caudate nucleus (Walker, 1940) were made and ultrathin

sections collected onto piloform-coated slot grids and counterstained with lead citrate. The DAB-labeled tissue sections were examined using a Zeiss EM10C electron microscope. Control sections processed as above except for the omission of the primary antibody did not contain DAB label upon electron microscopic examination.

Data analysis

The ultrastructural analysis of the DJ-1 immunostained macaque tissue sections was carried out as previously described (Bordelon et al., 2005; Muly et al., 2004a; Muly et al., 2004b). Regions of the grids containing neuropil were selected based on the presence of DAB label and adequate ultrastructural preservation. Fields of immunoreactive elements in the neuropil were randomly selected, and images were collected at a magnification of 31,500 using a Dualvision cooled CCD camera (1300 × 1030 pixels) and Digital Micrograph software (version 3.7.4, Gatan, Inc., Pleasanton, CA). On each micrograph, DAB-labeled profiles were identified and classified as spines, dendrites, terminals, axons, glia or unknown based on the established ultrastructural criteria (Bordelon et al., 2005; Peters et al., 1991). The number of immunoreactive profiles was tabulated and the data, which represents the distribution of randomly imaged labeled profiles observed in the neuropil (excluding the unknown profiles) were compared with a post-hoc Chi-square analysis as described previously (Bordelon et al., 2005; Muly et al., 2004a; Muly et al., 2004b; Pickel et al., 2006). This analysis was performed in multiple animals, and we have not observed significant inter-animal variability for DJ-1.

RESULTS

Generation and characterization of antibodies that specifically recognize evolutionally conserved epitopes in DJ-1

In order to compare the distribution of DJ-1 protein across species, we generated two anti-DJ-1 antibodies, P7C and P7F, against a conserved C-terminal peptide and the purified full-length recombinant protein of human DJ-1, respectively (Olzmann et al., 2004). To investigate the specificity and species cross-reactivity of our anti-DJ-1 antibodies and commercially available anti-DJ-1 antibody (KAM-SA100, Stressgen), immunoblot analysis was performed using extracts prepared from human, macaque, rat, wild type and DJ-1 knockout mouse brain tissues (Fig. 1A). All three antibodies recognized recombinant HA-tagged human DJ-1 as well as a single 20-kDa band, which corresponds well to the predicted molecular weight of endogenous DJ-1, in human and macaque brain extracts. As expected, the recombinant HA-tagged DJ-1 ran at a slightly higher molecular weight due to the additional 10 amino acids present in the HA-tag. Further characterization of these antibodies by immunohistochemistry demonstrated that all three DJ-1 antibodies showed similar staining patterns and primarily labeled astrocytes in human cingulate cortex (Fig. 1C). No immunoreactivity was observed when primary or secondary antibodies were omitted (data not shown).

As shown in Figure 1A, both P7C and P7F anti-DJ-1 antibodies, but not KAM-SA100 anti-DJ-1 antibody, also recognized a single 20-kDa band in rat and mouse brains. This 20-kDa band was absent in the extracts prepared from DJ-1 knockout mouse brain (Fig. 1B). Pre-absorption with purified recombinant human DJ-1 protein completely abolished the immunoreactivity of P7C, P7F, and KAM-SA100 (Fig. 1B), further confirming the specificity of these antibodies. Preabsorption with a carboxyl-terminal DJ-1 peptide (amino acids 171 −189) abolished the immunoreactivity of the P7C antibody, but not P7F or KAM-SA100, indicating that P7C recognizes an epitope distinct from that recognized by P7F and KAM-SA100. Together, these results indicate that P7C and P7F antibodies recognize different DJ-1 epitopes that are evolutionarily conserved in primate and rodent forms of DJ-1 protein. In contrast, the epitope recognized by the KAM-SA100 anti-DJ-1 antibody is only present in human and macaque DJ-1, but not in rodent DJ-1. Therefore, P7C and P7F antibodies are useful

tools for direct comparison of DJ-1 expression patterns between different species and were used in this study.

Species differences in the distribution of DJ-1 protein in human versus rat brain

Immunohistochemical analysis of DJ-1 expression in human cingulate cortex with P7C, P7F, or KAM-SA100 anti-DJ-1 antibodies resulted in similar staining patterns (Fig. 1, Fig. 2A-D, and additional data not shown). Diffuse DJ-1 immunostaining was observed across all cortical layers in human cingulate cortex (Fig. 2A). At higher magnification, DJ-1 staining was primarily localized in glial cells, in both gray matter (Fig. 2B) and white matter (Fig. 2C). DJ-1 label extended throughout the cell, including the cytoplasm, processes, and occasionally the nucleus. In addition, rare pyramidal neurons displayed weak DJ-1 immunoreactivity (Fig. 2D) and staining of cortical neuropil was also evident.

In contrast to the distribution of DJ-1 in human cortex, P7C or P7F anti-DJ-1 antibodies predominantly labeled neurons in rat brain (Fig. 2E-N). In the rat frontal cortex, the strongest immunoreactivity was observed within layer V pyramidal neurons (Fig. 2E-G) and moderate staining was present in neurons within layers II-III (Fig. 2E). A similar laminar distribution was seen in other areas of rat cortex including parietal, temporal, and retrosplenial (data not shown). In addition to the prominent staining of neurons, rare DJ-1-immunoreactive cells that appeared to be cortical glia were also observed (Fig. 2H). DJ-1 immunostaining was also found in rat striatum and substantia nigra. In the striatum, strong DJ-1 immunoreactivity was detected in large interneurons and moderate immunoreactivity was seen in medium spiny neurons (Fig. 2I-K). In addition, there was robust immunostaining of the neuropil. In the substantia nigra pars compacta and pars reticulata, neuronal perikarya and processes were enriched with DJ-1 immunoreactivity (Fig. 2L-M). The different patterns of DJ-1 immunostaining observed in human and rat with the same anti-DJ-1 antibodies strongly suggest that there are species differences in DJ-1 distribution in human versus rat brain.

To further confirm the specificity and cellular identity of the DJ-1 immunostaining, we performed dual immunofluorescence confocal microscopy in rat brain. DJ-1 distribution displayed substantial overlap with that of the neuronal marker NeuN in the regions examined, including the cortex, substantia nigra, and striatum (Fig. 3A). We also observed that many NeuN-immunoreactive neurons were not stained by DJ-1 antibodies, suggesting that the observed DJ-1 neuronal staining is specific. We found that DJ-1 is expressed in tyrosine hydroxylase-positive neurons in the substantia nigra pars compacta (Fig. 3B). In contrast, DJ-1 immunoreactivity showed very little overlap with the glial marker GFAP, although occasional DJ-1 immunoreactive astrocytes were observed in the white matter (Fig. 4).

Unfortunately, despite repeated attempts, double immunofluorescence labeling in human and macaque brains was unsuccessful due to high levels of autofluorescence and other technical difficulties. However, the morphologies of neurons and glia have been extensively described (Fairen et al., 1977; Jones, 1975; Lund, 1973; Lund and Boothe, 1975; Peters and Jones, 1984a; Peters and Jones, 1984b; Takato and Goldring, 1979). These studies have established criteria that allow for discrimination between several cell types, based on their unique morphologies (e.g. size and shape of the cell body and radiating processes). As described above, in human cortex, DJ-1 label was primarily observed in cells that exhibited characteristics of astrocytes, such as a small, centrally located ovoid cell body that tapered into radiating processes extending out into the neuropil (Fig. 2A and B). These were distinguishable from the occasionally observed, weakly immunostained cells that displayed characteristics of pyramidal neurons, including a conal, vertically elongated cell body with the hallmark large-apical dendrite extending towards the pial surface (Fig. 2C). The morphological analysis of the immunohistochemical staining in human and rat brains, combined with the dual

immunofluorescence labeling in rat brain, support species variation in the DJ-1 expression in human versus rat brain.

Differential DJ-1 expression in primate cortex versus substantia nigra and striatum

In an attempt to exclude the possibility that the observed differences between DJ-1 localization in rat and human brains might be due to artifact resulting from fixation and/or post-mortem interval, we performed immunostaining of the macaque brains. We found that the pattern of DJ-1 expression in macaque cortex was very similar to that of human cortex (Fig. 5A). DJ-1 immunoreactivity was prevalent in glial cells in both gray matter (Fig. 5B) and white matter (Fig. 5C). DJ-1 staining was also observed in neuropil and occasionally in some pyramidal neurons (Fig. 5D).

In contrast to the predominant glial expression of DJ-1 in macaque cortex, DJ-1 immunostaining was primarily neuronal in the macaque substantia nigra (Fig. 5H) and striatum (Fig. 5E). We observed DJ-1-immunoreactive large interneurons (Fig. 5E) interspersed among moderately stained medium spiny neurons in the striatum, (Fig. 5E and F). DJ-1 staining was also present in striatal neuropil and infrequently found in glia (Fig. 5G). Moderate DJ-1 immunolabeling was also observed in neurons in the substantia nigra pars compacta (Fig. 4H) and ventral tegmental area (Fig. 4I). Immunoreactivity was enriched in the neuronal perikarya and the neuronal processes descending into the substantia nigra pars reticulata. In addition to the nigral-striatal system, DJ-1 staining was also observed in neurons in other subcortical regions, including the hippocampus, amygdala, and thalamus (data not shown).

The DJ-1 immunostaining in macaque brain reveals differential expression of DJ-1 protein in the cortical versus subcortical regions. To determine if similar regional differences occur in human brain, we performed immunohistochemical analysis of human striatum and substantia nigra. In agreement with the DJ-1 distribution observed in the macaque (Fig. 5), DJ-1 immunoreactivity was primarily neuronal in the human subcortical regions examined (Fig. 6). DJ-1 labeling was seen in neuromelanin-positive as well as neuromelanin-negative neurons in the substantia nigra pars compacta (Fig. 6A and B) and reticulata (Fig. 6A and C). This finding suggests that as in rat nigra (Fig. 2 and 3), DJ-1 is expressed in human dopaminergic neurons. Similar to other PD-associated proteins, DJ-1 expression is not restricted to these dopaminergic neurons (D'Agata et al., 2002;Gandhi et al., 2006;Hsu et al., 1998;Mori et al., 2002;Stichel et al., 2000;Taymans et al., 2006). In addition, moderate DJ-1 immunoreactivity was seen within the medium spiny neurons in the striatum (Fig. 6D). Together, these results reveal regional differences in the distribution of DJ-1 protein in both human and macaque brains, and are the first to show neuronal expression in the primate substantia nigra and striatum.

DJ-1 is selectively enriched in primate striatal axons and synaptic compartments

Next, we used immunoelectron microscopy to determine the ultrastructural localization of DJ-1 in macaque brain. The striatum and prefrontal cortex were chosen for the ultrastructural analysis because both regions receive extensive dopaminergic input (Ciliax et al., 1999). Interestingly, nigrostriatal projections undergo selective degeneration in PD, whereas the mesocortical projections are relatively unaffected. Immunoelectron microscopic analysis revealed that in prefrontal cortex, DJ-1 immunoreactivity was predominantly found in glial cells (Fig. 7A and B), which is consistent with the immunohistochemical results obtained at the light microscopic level (Fig. 5A-C). DJ-1 immunoreactive glial processes were often wrapped around asymmetric synaptic contacts between axon terminals and dendritic spines (Fig. 7B). DJ-1 immunostaining was also commonly observed in neuronal dendrites (Fig. 7C and D) and very rarely in axons, presynaptic terminals, and dendrites (Data not shown). In the striatum, we most commonly observed DJ-1 label within axons (Fig. 8A and C). In addition, DJ-1 label was also seen to a lesser extent in other neuronal profiles, including dendrites (Fig.

8B and C), presynaptic terminals (Fig. 8D), dendritic spines (Fig. 8E), and glia (Fig. 8F). Similar staining patterns were observed with both the P7C and P7F DJ-1 antibodies and no immunoreactivity was observed in control sections processed in parallel when the primary antibody was omitted, confirming the specificity of our observations (data not shown).

To determine regional differences in the expression pattern of DJ-1, the relative distribution of DJ-1 immunoreactive profiles (Fig. 9) was determined and compared using a chi-square post-hoc analysis as described previously (Bordelon et al., 2005;Muly et al., 2004a;Muly et al., 2004b;Pickel et al., 2006). In layer III of the prefrontal cortex, we imaged 545 profiles in 229 micrographs representing 1,397 μm^2 and in the striatum we examined 657 profiles in 271 micrographs representing 1,654 μm^2. The relative distribution of DJ-1 in the neuropil differed significantly between the two regions ($\chi^2 = 194.303$; $p < 0.0001$). Post hoc testing revealed that all five neuropil elements (axon, presynaptic terminal, dendrite, dendritic spine, and glia) differed significantly between the striatum and prefrontal cortex, confirming our qualitative observations. In the cortex relative to the striatum, DJ-1 was found more often in dendrites (45.7% vs. 30.0%) and glia (38.9% vs. 15.7%). Conversely, in the striatum, DJ-1 was found more frequently in spines (6.3% vs. 2.8%), presynaptic terminals (5.8% vs. 2.8%) and axons (42.2% vs. 11.2%). These data reveal a profound difference between the neuropil distribution of DJ-1 in the prefrontal cortex and striatum. Furthermore, the selective enrichment of DJ-1 protein in striatal axons, presynaptic terminals, and dendritic spines implies an important physiological role for DJ-1 in striatal axonal and synaptic compartments.

DISCUSSION

Although inherited forms of PD are rare, studies of the familial PD gene products continue to provide valuable insights into the pathogenic mechanisms underlying the idiopathic form of PD. This is the first report of a direct comparison of the expression of familial PD-associated protein DJ-1 in the human, macaque, and rat brains, and the first study to use electron microscopy to explore the neuropil distribution of DJ-1. Our results have important implications for understanding the role of DJ-1 in normal physiology and in PD pathogenesis.

By using highly specific DJ-1 antibodies that recognize evolutionarily conserved epitopes, we found that, in contrast to the strong neuronal expression in the rat cortex, DJ-1 is primarily present in glia in human cortex, consistent with previous reports (Bandopadhyay et al., 2004; Meulener et al., 2005; Miller et al., 2005; Neumann et al., 2004). One possibility that might account for the observed differences between the DJ-1 expression in rat and human brains is artifact resulting from fixation and/or post-mortem interval. However, the fact that similar staining patterns were observed in both human and macaque brains strongly argues against this possibility and supports species variation in the expression patterns of DJ-1. A second possibility is that the DJ-1 distribution could be altered in aged human brain due to decreased proteasomal function. Although we cannot rule out an indirect effect, previous studies from our group and several others have found that wild-type DJ-1 does not undergo degradation by the proteasome (Miller et al., 2003; Moore et al., 2003; Olzmann et al., 2004). In addition, similar staining patterns were observed in all human (including a young case, age 34) and macaque brains, which included both young and aged brains, arguing against proteasomal deficit-induced accumulation of DJ-1. Unfortunately, additional young human cases were unavailable for a more quantitative biochemical and immunohistochemical analysis of DJ-1 protein levels. Finally, the use of two distinct anti-DJ-1 antibodies (P7C and P7F) that recognize both primate and rodent forms of DJ-1 protein provides strong support that the observed differential expression in primate versus rat brain does not result from differences in epitopes, but instead represents actual species differences in DJ-1 expression. This finding is interesting given the reported differences between the primate and rodent dopaminergic systems (Berger et al., 1991; Joel and Weiner, 2000).

The molecular mechanism by which loss-of-function mutations in DJ-1 induces dopaminergic neuronal degeneration is unclear. Our finding that in DJ-1 is expressed in neurons in subcortical regions of human and non-human primate brain suggests that DJ-1 has the potential to act directly within these susceptible neurons, instead of indirectly through regulation of surrounding glia. Several studies have demonstrated the involvement of DJ-1 in the cellular defense against oxidative stress (Kinumi et al., 2004; Martinat et al., 2004; Taira et al., 2004; Yokota et al., 2003; Zhou and Freed, 2005) and there is substantial evidence implicating oxidative stress in PD pathogenesis (Jenner, 2003). DJ-1 has also been shown to confer protection against a myriad of oxidative insults, including hydrogen peroxide and 1-methyl-4-phenylpyridinium (MPP^+) (Canet-Aviles et al., 2004; Taira et al., 2004; Yokota et al., 2003). Our results suggest that DJ-1 may be a key anti-oxidant in neurons.

One of the most intriguing aspects of PD pathology is the selective vulnerability of nigrostriatal dopaminergic neurons with respect to other dopaminergic nuclei. Although both the prefrontal cortex and the striatum receive dopaminergic innervation, the striatum receives a far denser projection and the input is from the substantia nigra pars compacta, which undergoes selective and extensive neurodegeneration in PD (Moore, 2003; Seamans and Yang, 2004). In addition, evidence suggests that dopaminergic neurodegeneration may begin with loss of striatal nerve terminals and a ‘dying back’ process (Dauer and Przedborski, 2003). Our quantitative electron microscopy study reveals a selective enrichment of DJ-1 protein in primate striatal axons, presynaptic terminals, and dendritic spines compared with the prefrontal cortex. Recently, Zhang et al. used qualitative post-embedding immunogold labeling and electron microscopy to show DJ-1 label in the mitochondrial matrix (Zhang et al., 2005). Immunogold labeling has the advantage of spatial resolution, but is less sensitive and is associated with increased noise when compared to the immunoperoxidase labeling used in the present study (Muly et al., 2004b). The experiments described in this paper are designed to identify the types of elements that contain DJ-1, but not the precise localization of DJ-1 within those elements. Consequently, the data presented here cannot speak to mitochondrial localization of DJ-1 in any significant way, although we have observed DJ-1 labeled mitochondria in our immunostained primate brain sections. The findings from our analysis of the neuropil distribution of DJ-1 support a selective role for DJ-1 within primate striatum, possibly in the maintenance of presynaptic axon integrity through reduction of cellular oxidative stress levels or through regulation of dopaminergic signaling.

In conclusion, our comprehensive analysis has revealed unexpected species as well as regional differences in the distribution of DJ-1 protein in human, macaque, and rat brains. Our finding that DJ-1 is selectively concentrated in striatal axons and presynaptic terminals suggests a role for DJ-1 in dopaminergic neurotransmission or a neuroprotective function of DJ-1 at the striatal terminals.

ACKNOWLEDGEMENTS

We thank Dr. Charles R. Gerfen and the Neurological Disease and Stroke/University of California Los Angeles Repository for Parkinson's disease Mouse Models for providing the DJ-1 knockout mice. This work was supported by grants from National Institutes of Health (NS054597, NS047199, NS050650, AG021489, MH01194, and RR00165).

LITERATURE CITED

Abou-Sleiman PM, Healy DG, Wood NW. Causes of Parkinson's disease: genetics of DJ-1. Cell Tissue Res 2004;318(1):185–188. [PubMed: 15503154]

Bader V, Ran Zhu X, Lubbert H, Stichel CC. Expression of DJ-1 in the adult mouse CNS. Brain Res 2005;1041(1):102–111. [PubMed: 15804505]

Bandopadhyay R, Kingsbury AE, Cookson MR, Reid AR, Evans IM, Hope AD, Pittman AM, Lashley T, Canet-Aviles R, Miller DW, McLendon C, Strand C, Leonard AJ, Abou-Sleiman PM, Healy DG, Ariga H, Wood NW, de Silva R, Revesz T, Hardy JA, Lees AJ. The expression of DJ-1 (PARK7) in normal human CNS and idiopathic Parkinson's disease. Brain 2004;127(Pt 2):420–430. [PubMed: 14662519]

Berger B, Gaspar P, Verney C. Dopaminergic innervation of the cerebral cortex: unexpected differences between rodents and primates. Trends Neurosci 1991;14(1):21–27. [PubMed: 1709528]

Bonifati V, Oostra BA, Heutink P. Linking DJ-1 to neurodegeneration offers novel insights for understanding the pathogenesis of Parkinson's disease. J Mol Med 2004;82(3):163–174. [PubMed: 14712351]

Bonifati V, Rizzu P, van Baren MJ, Schaap O, Breedveld GJ, Krieger E, Dekker MC, Squitieri F, Ibanez P, Joosse M, van Dongen JW, Vanacore N, van Swieten JC, Brice A, Meco G, van Duijn CM, Oostra BA, Heutink P. Mutations in the DJ-1 gene associated with autosomal recessive early-onset parkinsonism. Science 2003;299(5604):256–259. [PubMed: 12446870]

Bordelon JR, Smith Y, Nairn AC, Colbran RJ, Greengard P, Muly EC. Differential Localization of Protein Phosphatase-1{alpha}, {beta} and {gamma}1 Isoforms in Primate Prefrontal Cortex. Cereb Cortex. 2005

Canet-Aviles RM, Wilson MA, Miller DW, Ahmad R, McLendon C, Bandyopadhyay S, Baptista MJ, Ringe D, Petsko GA, Cookson MR. The Parkinson's disease protein DJ-1 is neuroprotective due to cysteine-sulfinic acid-driven mitochondrial localization. Proc Natl Acad Sci U S A 2004;101(24): 9103–9108. [PubMed: 15181200]

Chen L, Cagniard B, Mathews T, Jones S, Koh HC, Ding Y, Carvey PM, Ling Z, Kang UJ, Zhuang X. Age-dependent motor deficits and dopaminergic dysfunction in DJ-1 null mice. J Biol Chem 2005;280 (22):21418–21426. [PubMed: 15799973]

Chin LS, Li L, Ferreira A, Kosik KS, Greengard P. Impairment of axonal development and of synaptogenesis in hippocampal neurons of synapsin I-deficient mice. Proc Natl Acad Sci U S A 1995;92(20):9230–9234. [PubMed: 7568107]

Chin LS, Vavalle JP, Li L. Staring, a novel E3 ubiquitin-protein ligase that targets syntaxin 1 for degradation. J Biol Chem 2002;277(38):35071–35079. [PubMed: 12121982]

Choi J, Levey AI, Weintraub ST, Rees HD, Gearing M, Chin LS, Li L. Oxidative modifications and down-regulation of ubiquitin carboxyl-terminal hydrolase L1 associated with idiopathic Parkinson's and Alzheimer's diseases. J Biol Chem 2004;279(13):13256–13264. [PubMed: 14722078]

Choi J, Sullards MC, Olzmann JA, Rees HD, Weintraub ST, Bostwick DE, Gearing M, Levey AI, Chin LS, Li L. Oxidative damage of DJ-1 is linked to sporadic Parkinson and Alzheimer diseases. J Biol Chem 2006;281(16):10816–10824. [PubMed: 16517609]

Ciliax BJ, Drash GW, Staley JK, Haber S, Mobley CJ, Miller GW, Mufson EJ, Mash DC, Levey AI. Immunocytochemical localization of the dopamine transporter in human brain. J Comp Neurol 1999;409(1):38–56. [PubMed: 10363710]

Cookson MR. The biochemistry of Parkinson's disease. Annu Rev Biochem 2005;74:29–52. [PubMed: 15952880]

D'Agata V, Zhao W, Pascale A, Zohar O, Scapagnini G, Cavallaro S. Distribution of parkin in the adult rat brain. Prog Neuropsychopharmacol Biol Psychiatry 2002;26(3):519–527. [PubMed: 11999903]

Dauer W, Przedborski S. Parkinson's disease: mechanisms and models. Neuron 2003;39(6):889–909. [PubMed: 12971891]

Debus E, Weber K, Osborn M. Monoclonal antibodies specific for glial fibrillary acidic (GFA) protein and for each of the neurofilament triplet polypeptides. Differentiation 1983;25(2):193–203. [PubMed: 6198232]

Fairen A, Peters A, Saldanha J. A new procedure for examining Golgi impregnated neurons by light and electron microscopy. J Neurocytol 1977;6(3):311–337. [PubMed: 71343]

Gandhi S, Muqit MM, Stanyer L, Healy DG, Abou-Sleiman PM, Hargreaves I, Heales S, Ganguly M, Parsons L, Lees AJ, Latchman DS, Holton JL, Wood NW, Revesz T. PINK1 protein in normal human brain and Parkinson's disease. Brain 2006;129(Pt 7):1720–1731. [PubMed: 16702191]

Goldberg MS, Pisani A, Haburcak M, Vortherms TA, Kitada T, Costa C, Tong Y, Martella G, Tscherter A, Martins A, Bernardi G, Roth BL, Pothos EN, Calabresi P, Shen J. Nigrostriatal dopaminergic

deficits and hypokinesia caused by inactivation of the familial Parkinsonism-linked gene DJ-1. Neuron 2005;45(4):489–496. [PubMed: 15721235]

Hardman CD, Henderson JM, Finkelstein DI, Horne MK, Paxinos G, Halliday GM. Comparison of the basal ganglia in rats, marmosets, macaques, baboons, and humans: volume and neuronal number for the output, internal relay, and striatal modulating nuclei. J Comp Neurol 2002;445(3):238–255. [PubMed: 11920704]

Hsu LJ, Mallory M, Xia Y, Veinbergs I, Hashimoto M, Yoshimoto M, Thal LJ, Saitoh T, Masliah E. Expression pattern of synucleins (non-Abeta component of Alzheimer's disease amyloid precursor protein/alpha-synuclein) during murine brain development. J Neurochem 1998;71(1):338–344. [PubMed: 9648883]

Huai Q, Sun Y, Wang H, Chin LS, Li L, Robinson H, Ke H. Crystal structure of DJ-1/RS and implication on familial Parkinson's disease. FEBS Lett 2003;549(1−3):171–175. [PubMed: 12914946]

Jenner P. Oxidative stress in Parkinson's disease. Ann Neurol 2003;53(Suppl 3):S26–36. [PubMed: 12666096]discussion S36−28

Joel D, Weiner I. The connections of the dopaminergic system with the striatum in rats and primates: an analysis with respect to the functional and compartmental organization of the striatum. Neuroscience 2000;96(3):451–474. [PubMed: 10717427]

Jones EG. Varieties and distribution of non-pyramidal cells in the somatic sensory cortex of the squirrel monkey. J Comp Neurol 1975;160(2):205–267. [PubMed: 803518]

Kim RH, Smith PD, Aleyasin H, Hayley S, Mount MP, Pownall S, Wakeham A, You-Ten AJ, Kalia SK, Horne P, Westaway D, Lozano AM, Anisman H, Park DS, Mak TW. Hypersensitivity of DJ-1-deficient mice to 1-methyl-4-phenyl-1,2,3,6-tetrahydropyrindine (MPTP) and oxidative stress. Proc Natl Acad Sci U S A 2005;102(14):5215–5220. [PubMed: 15784737]

Kinumi T, Kimata J, Taira T, Ariga H, Niki E. Cysteine-106 of DJ-1 is the most sensitive cysteine residue to hydrogen peroxide-mediated oxidation in vivo in human umbilical vein endothelial cells. Biochem Biophys Res Commun 2004;317(3):722–728. [PubMed: 15081400]

Kotaria N, Hinz U, Zechel S, von Bohlen Und Halbach O. Localization of DJ-1 protein in the murine brain. Cell Tissue Res 2005:1–5.

Lang AE, Lozano AM. Parkinson's disease. First of two parts. N Engl J Med 1998a;339(15):1044–1053. [PubMed: 9761807]

Lang AE, Lozano AM. Parkinson's disease. Second of two parts. N Engl J Med 1998b;339(16):1130–1143. [PubMed: 9770561]

Lee SJ, Kim SJ, Kim IK, Ko J, Jeong CS, Kim GH, Park C, Kang SO, Suh PG, Lee HS, Cha SS. Crystal structures of human DJ-1 and Escherichia coli Hsp31, which share an evolutionarily conserved domain. J Biol Chem 2003;278(45):44552–44559. [PubMed: 12939276]

Li Y, Chin LS, Weigel C, Li L. Spring, a novel RING finger protein that regulates synaptic vesicle exocytosis. J Biol Chem 2001;276(44):40824–40833. [PubMed: 11524423]

Lund JS. Organization of neurons in the visual cortex, area 17, of the monkey (Macaca mulatta). J Comp Neurol 1973;147(4):455–496. [PubMed: 4122705]

Lund JS, Boothe RG. Interlaminar connections and pyramidal neuron organisation in the visual cortex, area 17, of the Macaque monkey. J Comp Neurol 1975;159(3):305–334.

Martinat C, Shendelman S, Jonason A, Leete T, Beal MF, Yang L, Floss T, Abeliovich A. Sensitivity to oxidative stress in DJ-1-deficient dopamine neurons: an ES- derived cell model of primary parkinsonism. PLoS Biol 2004;2(11):e327. [PubMed: 15502868]

Meulener MC, Graves CL, Sampathu DM, Armstrong-Gold CE, Bonini NM, Giasson BI. DJ-1 is present in a large molecular complex in human brain tissue and interacts with alpha-synuclein. J Neurochem 2005;93(6):1524–1532. [PubMed: 15935068]

Miller DW, Ahmad R, Hague S, Baptista MJ, Canet-Aviles R, McLendon C, Carter DM, Zhu PP, Stadler J, Chandran J, Klinefelter GR, Blackstone C, Cookson MR. L166P mutant DJ-1, causative for recessive Parkinson's disease, is degraded through the ubiquitin-proteasome system. J Biol Chem 2003;278(38):36588–36595. [PubMed: 12851414]

Miller DW, Wilson CR, Kaleem MA, Blackinton J, Cookson MR. Identification of the epitope of a monoclonal antibody to DJ-1. Neurosci Lett 2005;374(3):203–206. [PubMed: 15663963]

Moore DJ, West AB, Dawson VL, Dawson TM. Molecular pathophysiology of Parkinson's disease. Annu Rev Neurosci 2005;28:57–87. [PubMed: 16022590]

Moore DJ, Zhang L, Dawson TM, Dawson VL. A missense mutation (L166P) in DJ-1, linked to familial Parkinson's disease, confers reduced protein stability and impairs homo-oligomerization. J Neurochem 2003;87(6):1558–1567. [PubMed: 14713311]

Moore RY. Organization of midbrain dopamine systems and the pathophysiology of Parkinson's disease. Parkinsonism Relat Disord 2003;9(Suppl 2):S65–71. [PubMed: 12915070]

Mori F, Tanji K, Yoshimoto M, Takahashi H, Wakabayashi K. Immunohistochemical comparison of alpha- and beta-synuclein in adult rat central nervous system. Brain Res 2002;941(1−2):118–126. [PubMed: 12031554]

Mullen RJ, Buck CR, Smith AM. NeuN, a neuronal specific nuclear protein in vertebrates. Development 1992;116(1):201–211. [PubMed: 1483388]

Muly EC, Allen P, Mazloom M, Aranbayeva Z, Greenfield AT, Greengard P. Subcellular distribution of neurabin immunolabeling in primate prefrontal cortex: comparison with spinophilin. Cereb Cortex 2004a;14(12):1398–1407. [PubMed: 15217898]

Muly EC, Maddox M, Smith Y. Distribution of mGluR1alpha and mGluR5 immunolabeling in primate prefrontal cortex. J Comp Neurol 2003;467(4):521–535. [PubMed: 14624486]

Muly EC, Smith Y, Allen P, Greengard P. Subcellular distribution of spinophilin immunolabeling in primate prefrontal cortex: localization to and within dendritic spines. J Comp Neurol 2004b;469(2): 185–197. [PubMed: 14694533]

Muly EC, Szigeti K, Goldman-Rakic PS. D1 receptor in interneurons of macaque prefrontal cortex: distribution and subcellular localization. J Neurosci 1998;18(24):10553–10565. [PubMed: 9852592]

Neumann M, Muller V, Gorner K, Kretzschmar HA, Haass C, Kahle PJ. Pathological properties of the Parkinson's disease-associated protein DJ-1 in alpha-synucleinopathies and tauopathies: relevance for multiple system atrophy and Pick's disease. Acta Neuropathol (Berl) 2004;107(6):489–496. [PubMed: 14991385]

Offe K, Dodson SE, Shoemaker JT, Fritz JJ, Gearing M, Levey AI, Lah JJ. The lipoprotein receptor LR11 regulates amyloid beta production and amyloid precursor protein traffic in endosomal compartments. J Neurosci 2006;26(5):1596–1603. [PubMed: 16452683]

Olzmann JA, Brown K, Wilkinson KD, Rees HD, Huai Q, Ke H, Levey AI, Li L, Chin LS. Familial Parkinson's disease-associated L166P mutation disrupts DJ-1 protein folding and function. J Biol Chem 2004;279(9):8506–8515. [PubMed: 14665635]

Peters, A.; Jones, EG., editors. Cellular Components of the Cerebral Cortex. 1. Plenum; New York: 1984a.

Peters, A.; Jones, EG., editors. Functional Properties of Cortical Cells. 2. Plenum; New York: 1984b.

Peters, A.; Palay, SL.; Webster, HD. The fine structure of the nervous system: neurons and their supporting cells. Oxford University Press; New York: 1991.

Petrides M, Pandya DN. Comparative cytoarchitectonic analysis of the human and the macaque ventrolateral prefrontal cortex and corticocortical connection patterns in the monkey. Eur J Neurosci 2002;16(2):291–310. [PubMed: 12169111]

Pickel VM, Chan J, Kearn CS, Mackie K. Targeting dopamine D2 and cannabinoid-1 (CB1) receptors in rat nucleus accumbens. J Comp Neurol 2006;495(3):299–313. [PubMed: 16440297]

Seamans JK, Yang CR. The principal features and mechanisms of dopamine modulation in the prefrontal cortex. Prog Neurobiol 2004;74(1):1–58. [PubMed: 15381316]

Smiley JF, Levey AI, Ciliax BJ, Goldman-Rakic PS. D1 dopamine receptor immunoreactivity in human and monkey cerebral cortex: predominant and extrasynaptic localization in dendritic spines. Proc Natl Acad Sci U S A 1994;91(12):5720–5724. [PubMed: 7911245]

Stichel CC, Augustin M, Kuhn K, Zhu XR, Engels P, Ullmer C, Lubbert H. Parkin expression in the adult mouse brain. Eur J Neurosci 2000;12(12):4181–4194. [PubMed: 11122330]

Taira T, Saito Y, Niki T, Iguchi-Ariga SM, Takahashi K, Ariga H. DJ-1 has a role in antioxidative stress to prevent cell death. EMBO Rep 2004;5(2):213–218. [PubMed: 14749723]

Takato M, Goldring S. Intracellular marking with lucifer yellow CH and horseradish peroxidase of cells electrophysiologically characterized as glia in the cerebral cortex of the cat. J Comp Neurol 1979;186 (2):173–188. [PubMed: 87405]

Tao X, Tong L. Crystal structure of human DJ-1, a protein associated with early onset Parkinson's disease. J Biol Chem 2003;278(33):31372–31379. [PubMed: 12761214]

Taymans JM, Van den Haute C, Baekelandt V. Distribution of PINK1 and LRRK2 in rat and mouse brain. J Neurochem. 2006

Vila M, Przedborski S. Genetic clues to the pathogenesis of Parkinson's disease. Nat Med 2004;10 (Suppl):S58–62. [PubMed: 15272270]

Walker A. A cytoarchitectural study of the prefrontal area of the macaque monkey. J Comp Neurol 1940;73:59–86.

Yokota T, Sugawara K, Ito K, Takahashi R, Ariga H, Mizusawa H. Down regulation of DJ-1 enhances cell death by oxidative stress, ER stress, and proteasome inhibition. Biochem Biophys Res Commun 2003;312(4):1342–1348. [PubMed: 14652021]

Zhang L, Shimoji M, Thomas B, Moore DJ, Yu SW, Marupudi NI, Torp R, Torgner IA, Ottersen OP, Dawson TM, Dawson VL. Mitochondrial localization of the Parkinson's disease related protein DJ-1: implications for pathogenesis. Hum Mol Genet 2005;14(14):2063–2073. [PubMed: 15944198]

Zhang W, Basile AS, Gomeza J, Volpicelli LA, Levey AI, Wess J. Characterization of central inhibitory muscarinic autoreceptors by the use of muscarinic acetylcholine receptor knock-out mice. J Neurosci 2002;22(5):1709–1717. [PubMed: 11880500]

Zhou W, Freed CR. DJ-1 up-regulates glutathione synthesis during oxidative stress and inhibits A53T alpha-synuclein toxicity. J Biol Chem 2005;280(52):43150–43158. [PubMed: 16227205]

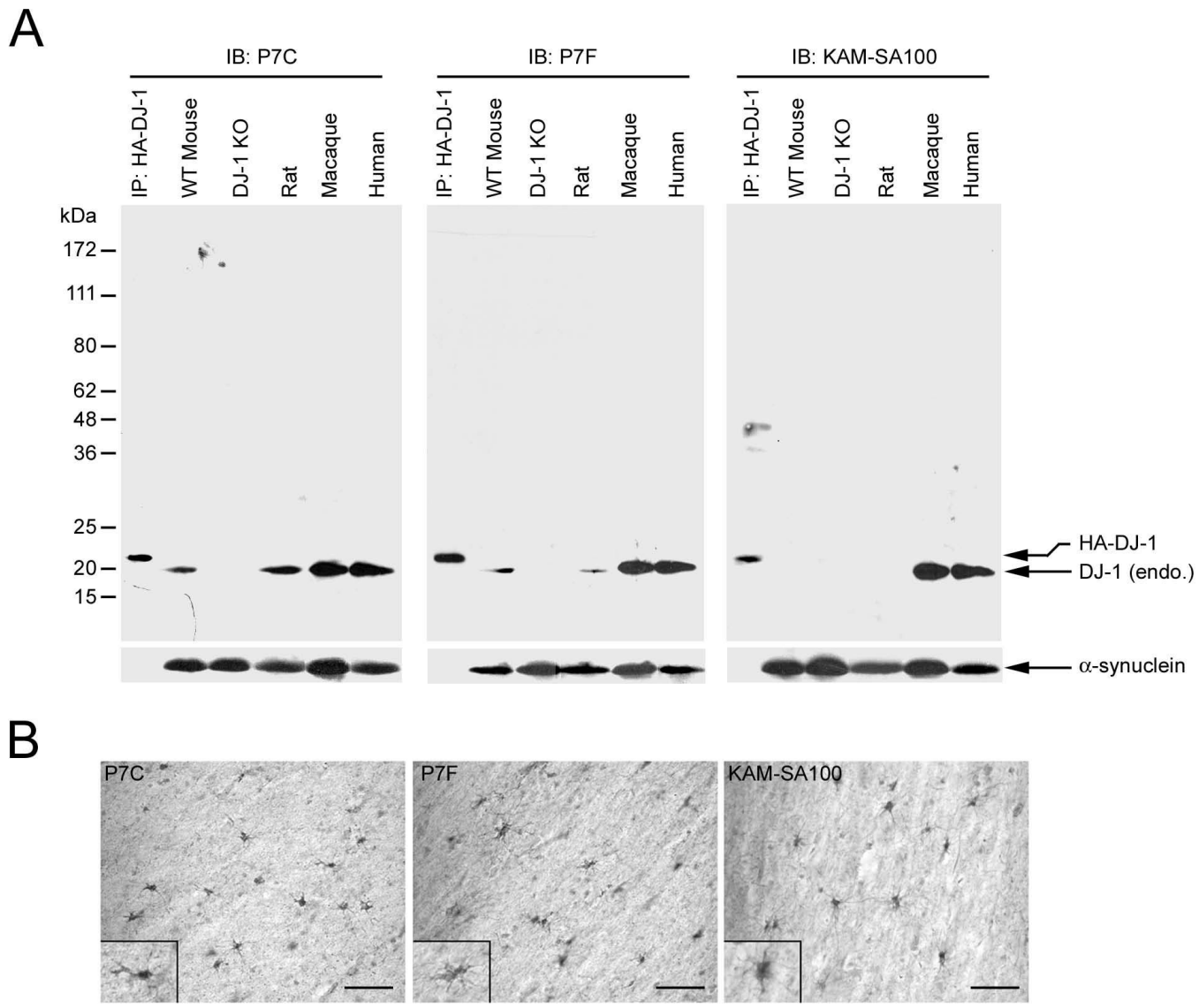

Fig. 1.

Characterization of anti-DJ-1 antibodies by Western blot and immunohistochemical analysis. (A) Equal amounts of homogenates (50 μg protein per lane) from wild-type (WT) mouse brain, DJ-1 knockout (KO) mouse brain, rat brain, macaque cortex, and human cortex were separated by SDS-PAGE and analyzed by immunoblotting (IB) with anti-DJ-1 antibodies P7C, P7F, or SA100 (KAM-SA100, Stressgen) and anti-α-synuclein antibodies as indicated. Immunoprecipitated HA-tagged human DJ-1 protein was used as a positive control. (B) Homogenates of macaque cortex (50 μg protein per lane) were resolved by SDS-PAGE and analyzed by immunoblotting. Anti-DJ-1 antibodies were preabsorbed for 2 h with 50 μg of synthetic human DJ-1 carboxyl-terminal peptide (DJ-1 C-Peptide, amino acids 171−189) or purified recombinant human DJ-1 (DJ-1 protein) as indicated, prior to immunoblotting. (C) Immunohistochemical analysis of DJ-1 protein distribution in human cortical tissues using P7C, P7F, or SA100 demonstrates similar labeling of astrocytes. *Scale bar = 50 μm*.

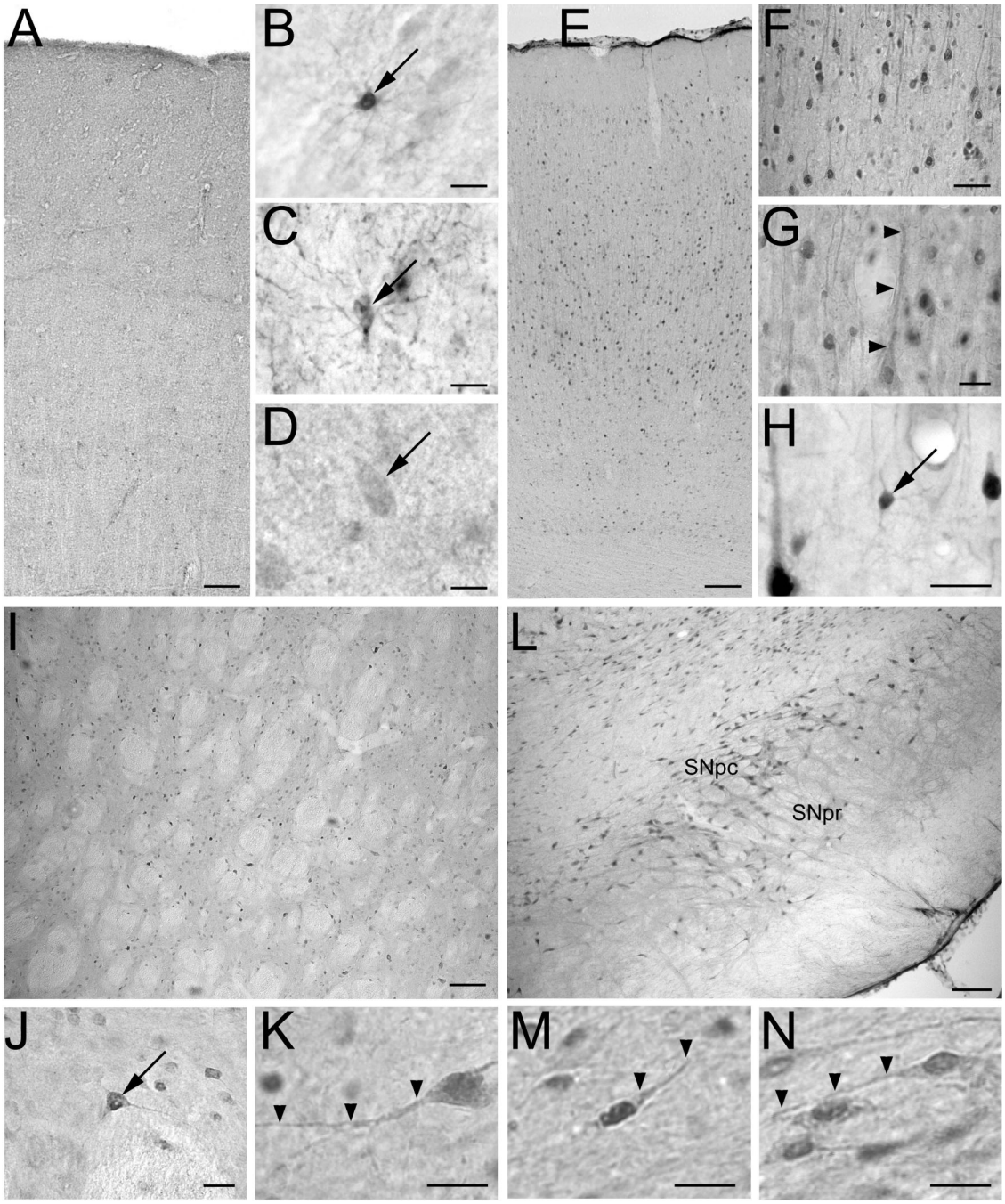

Fig. 2.

Immunohistochemical analysis reveals species differences in the distribution of DJ-1 protein in human versus rat brain. In the human brain (A-D), DJ-1 immunostaining was relatively evenly distributed across all cortical layers (A). At higher magnification, DJ-1 immunoreactivity was observed in glia in human cortical gray matter (B) and white matter (C). Very few neurons were labeled, but occasionally weak DJ-1 label was seen in human cortical neurons (D). In the rat brain (E-N), intense DJ-1 immunostaining was observed in neurons throughout the frontal cortex (E), with particularly strong label occurring in layer V. Neurons were also strongly labeled in layer II (F). The hallmark apical dendrite of some pyramidal neurons was visibly stained (G, *arrowheads*), and DJ-1 was also infrequently seen in cortical

glia (H). DJ-1 immunoreactivity was present in neurons throughout the rat striatum (I-K) and substantia nigra (L-N). At higher magnification, DJ-1 label was observed in the nucleus, cytoplasm, and processes of neurons with layer V of the frontal cortex (G, *arrowheads*), the striatum (J and K, *arrowheads*), substantia nigra pars compacta (M, *arrowheads*), and substantia nigra pars reticulata (N, *arrowheads*). SNpc, substantia nigra pars compacta; SNpr, substantia nigra pars reticulata. Scale bar = 20 μm in B-D, G, H, J, K, M, and N; 50 μm in F; 100 μm in A, E, I, and L.

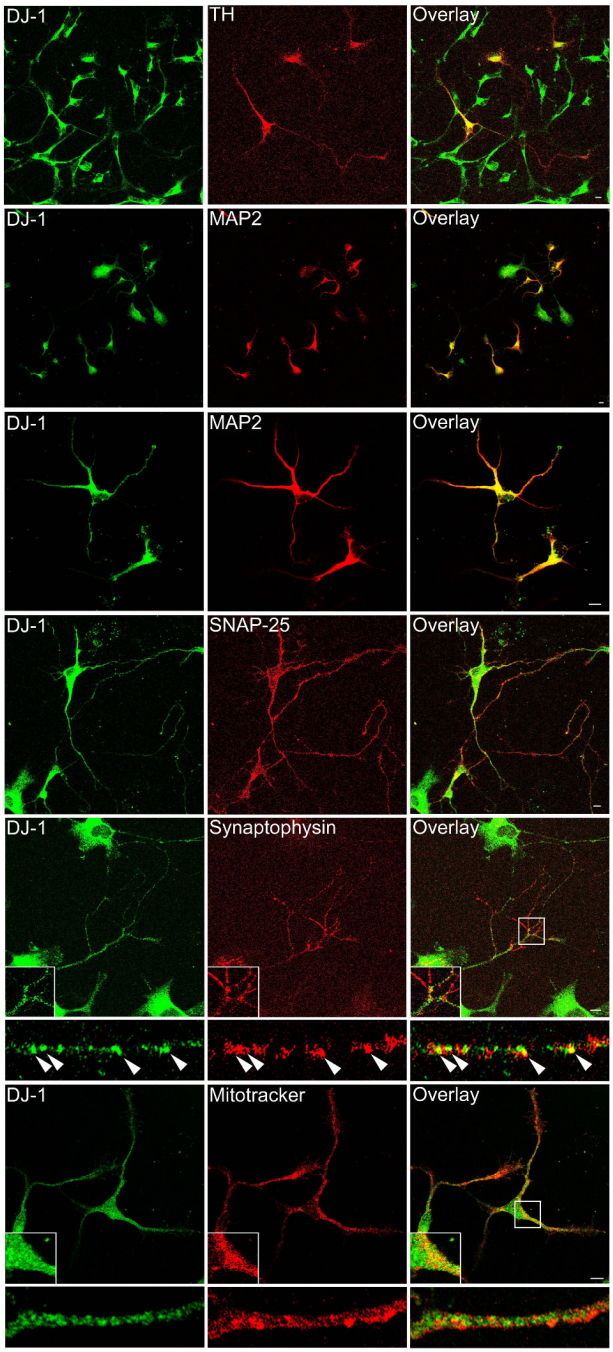

Fig. 3.

DJ-1 expression in dopaminergic neurons as well as in other neurons in rat brain. Rat brain sections were double stained with anti-DJ-1 antibody and antibodies against NeuN or tyrosine hydroxylase (TH) as indicated. DJ-1 label was observed in NeuN-immunoreactive neurons in the cortex, striatum, and substantia nigra (A, *arrowheads).* In addition, DJ-1 antibodies stained nigral, tyrosine hydroxylase-immunoreactive neurons (B, *arrowheads*). There are also many NeuN-immunoreactive neurons that were not labeled by DJ-1 antibodies (A, *open arrowheads*). DJ-1 immunostaining was occasionally observed in white matter glia, which were unstained by NeuN antibodies (A, *arrows*). Superimposed images (overlay) demonstrate the overlap in the expression patterns of DJ-1 with NeuN or TH. *Scale bar = 50 μm.*

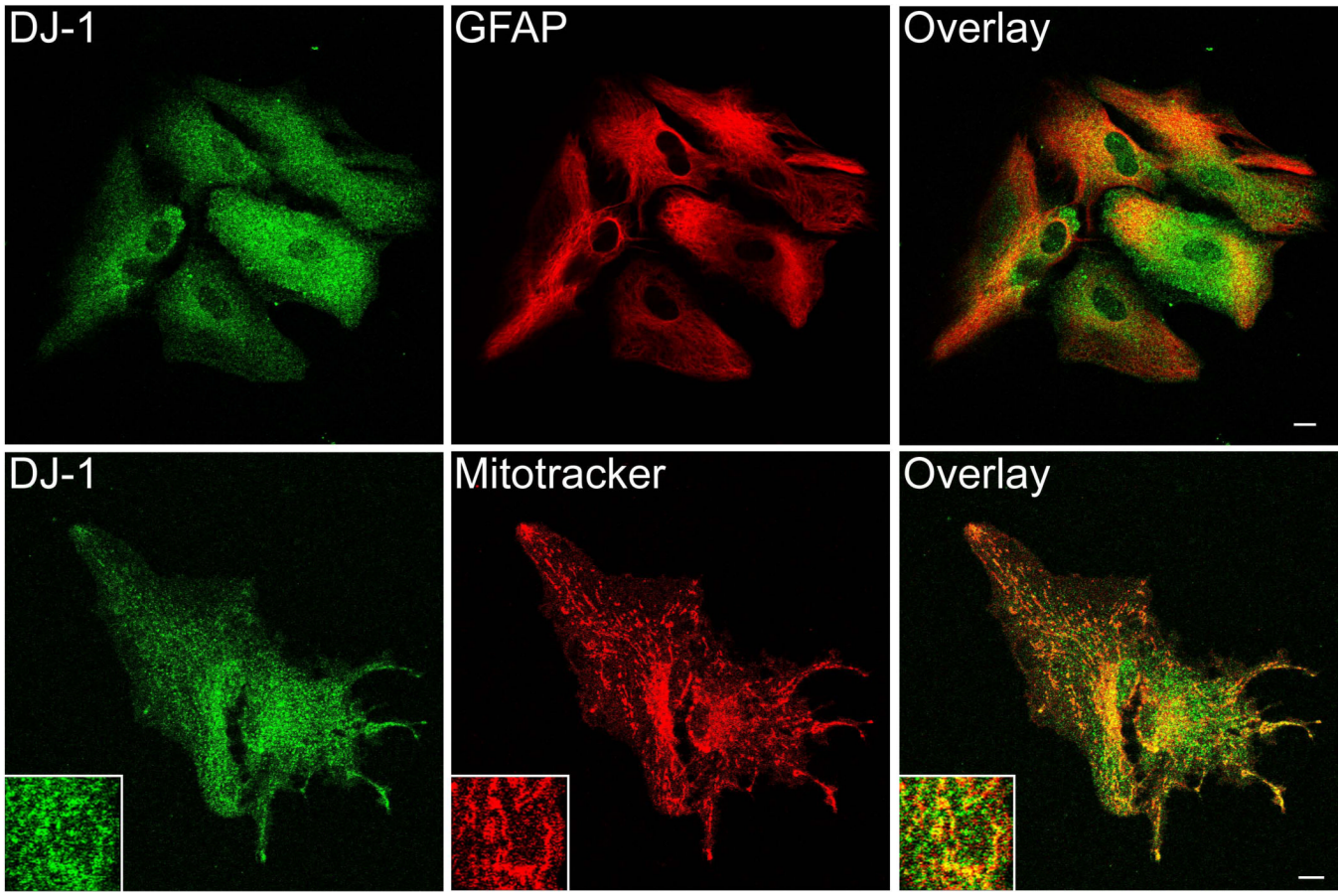

Fig 4.

Comparison of DJ-1 and GFAP immunostaining in rat brain by dual immunofluorescence confocal microscopy. Rat brain sections were double stained with anti-DJ-1 and anti-GFAP antibodies. DJ-1-immunoreactive cells in the cortex, striatum, and substantia nigra were not labeled by GFAP antibodies (*arrows*). DJ-1 immunostaining was absent from most GFAP-immunoreactive astrocytes (*open arrows*), except occasional astrocytes in the white matter (*arrowheads*). Superimposed images (overlay) show the distributions of these two proteins and their overlap. *Scale bar = 50 μm*.

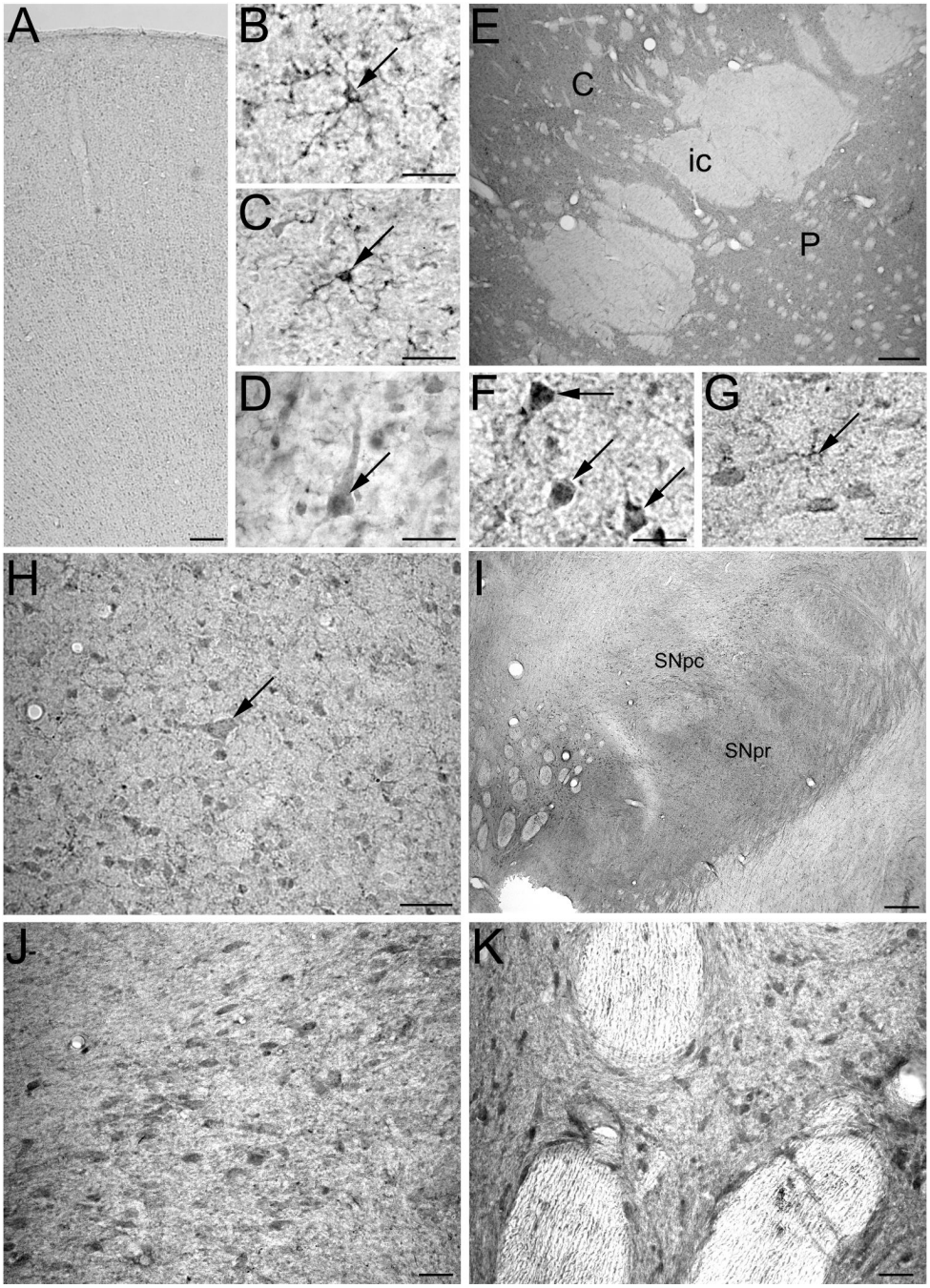

Fig. 5.

DJ-1 is expressed in macaque nigral and striatal neurons. DJ-1 immunostaining was distributed across all cortical layers within macaque frontal cortex (A). At higher magnification, DJ-1 immunoreactivity was found in glial cells in the cortical gray matter (B) and white matter (C), as well as in some pyramidal neurons (D). The macaque striatum (E) displays intense DJ-1 immunostaining, with immunoreactivity in medium spiny neurons (F), large interneurons (E, *arrow*), and some glial cells (G). DJ-1 immunostaining is also found in neurons in the substantia nigra pars compacta and their processes (H) as well as in neuronal perikarya in the ventral tegmental area (I). Scale bar = 20 μm in B-D, F, and G; 50 μm in E, H, and I; 100 μm in A.

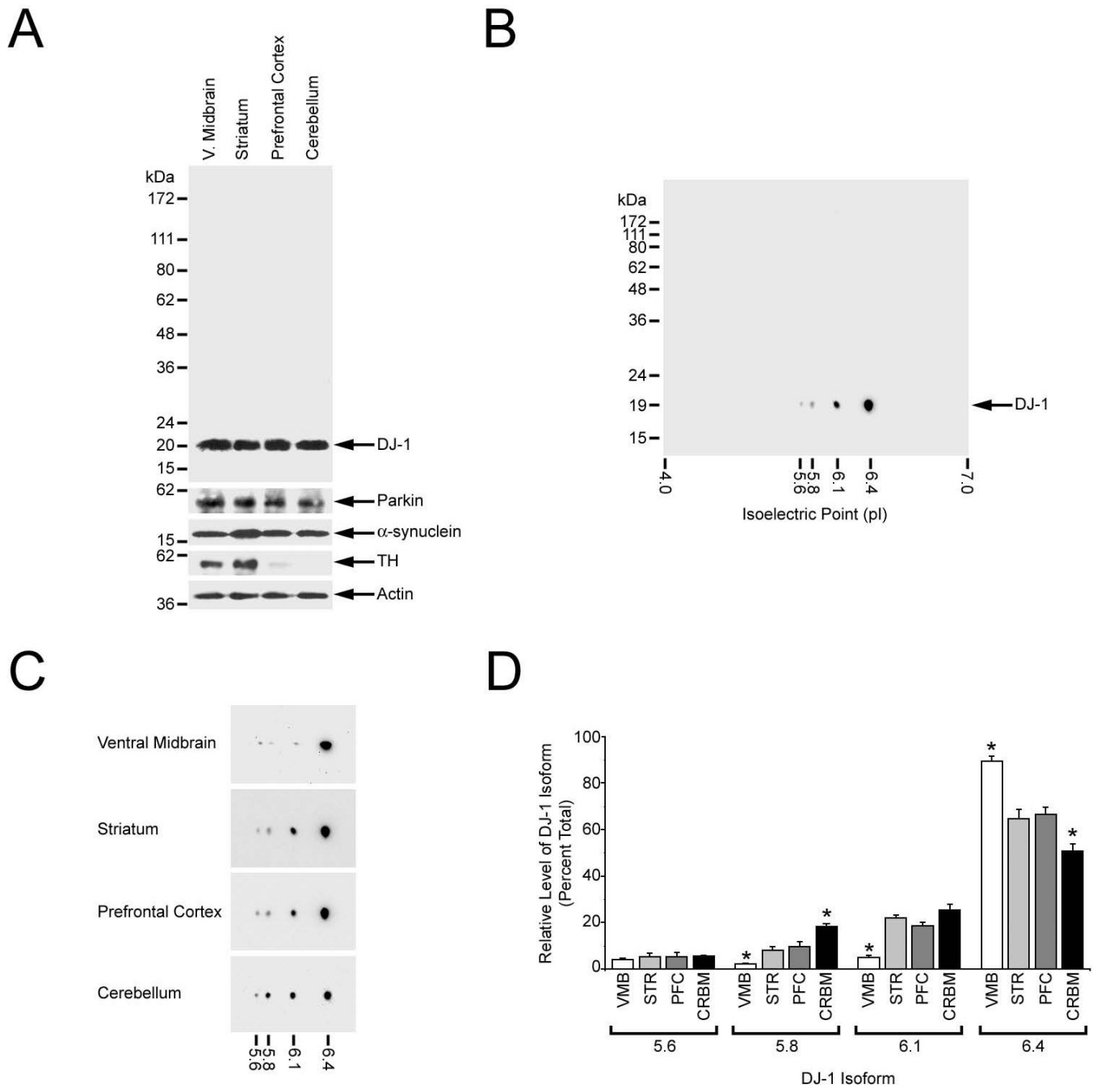

Fig. 6.

Immunohistochemical analysis reveals DJ-1 expression in human nigral and striatal neurons. DJ-1 protein is expressed in neurons throughout the human substantia nigra (A). In the substantia nigra pars compacta (B) and parts reticulata (C) DJ-1 immunostaining was observed in the perikarya and neurites. At higher magnification, DJ-1 immunoreactivity can be seen in neuromelanin-positive (D, *arrowhead*) as well as in neuromelanin-negative neurons (D). In human striatum (E and F), DJ-1 protein appears to be moderately expressed in most medium spiny neurons. Scale bar = 25 μm in D and F; 50 μm in E; 100 μm in B and C; 250 μm in A.

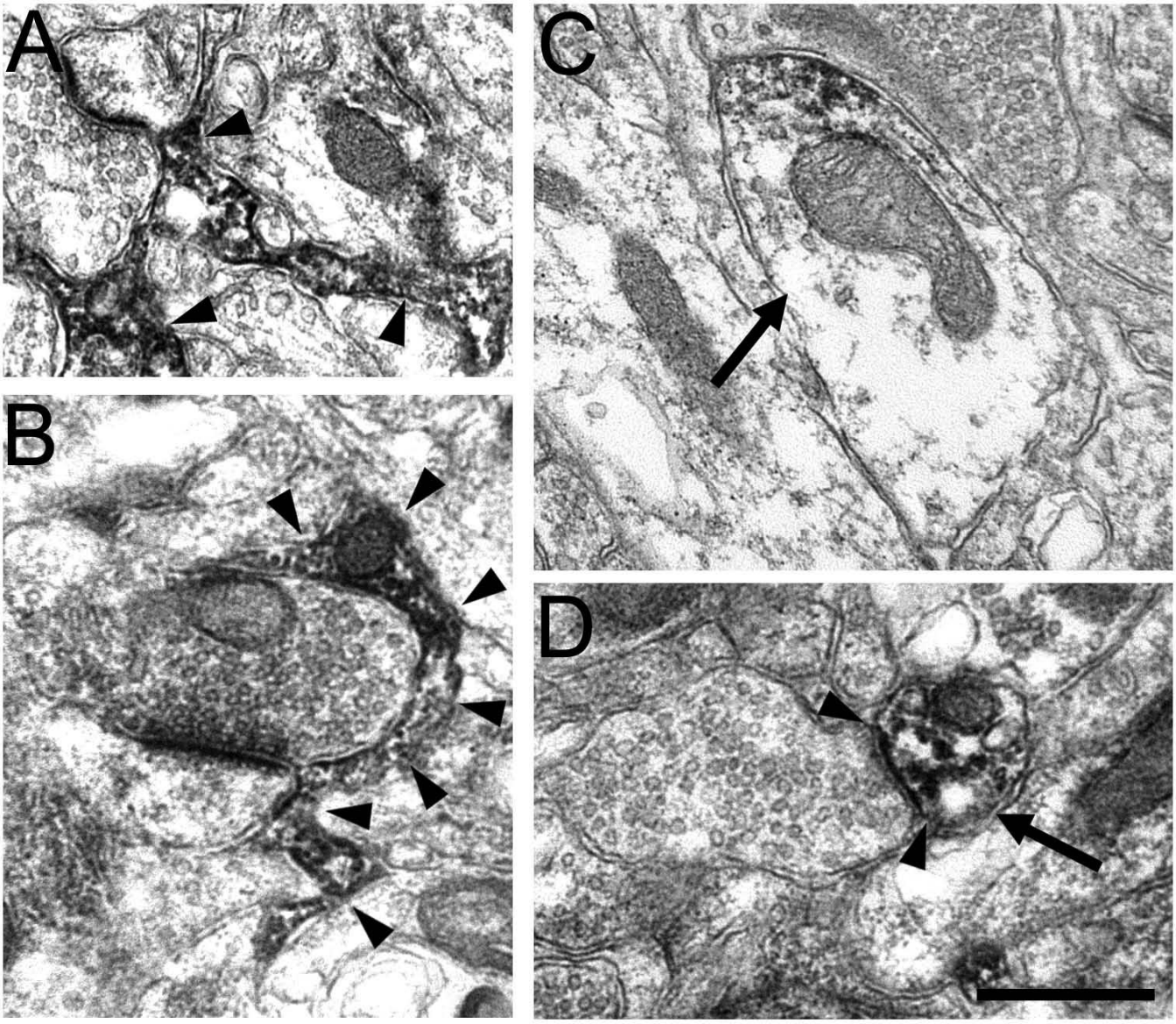

Fig. 7.

Electron micrographs illustrating the localization of DJ-1 in the neuropil of macaque monkey prefrontal cortex. DJ-1 label was primarily observed in glia (A and B, *arrowheads*) and dendrites (C and D, *arrows*). Glial profiles were irregularly shaped and often wrapped around asymmetric synaptic contacts. Some labeled dendritic profiles received asymmetric synaptic contacts (D, *arrowheads*). *Scale bar = 0.5 μm*.

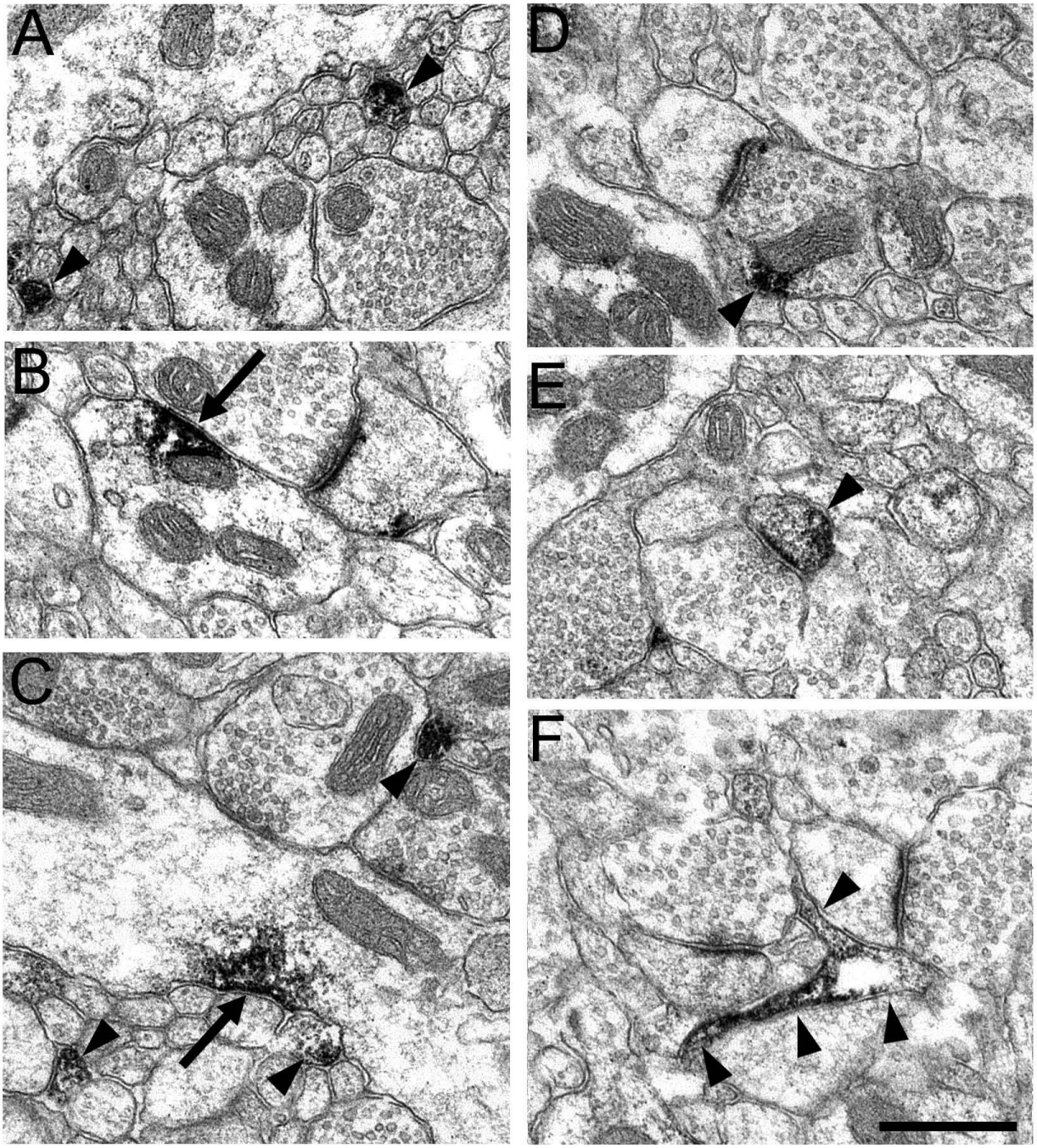

Fig. 8.

Electron micrographs illustrating the localization of DJ-1 in the neuropil of macaque monkey striatum. DJ-1 label was observed in all types of neuronal profiles, including axons (A and C, *arrowheads*), dendrites (B and C, *arrows*), presynaptic terminals (D, *arrowhead*), dendritic spines (E, *arrowhead*), and glia (F, *arrowheads*). Glial profiles were irregularly shaped and often observed in close proximity to synapses. *Scale bar = 0.5 μm*.

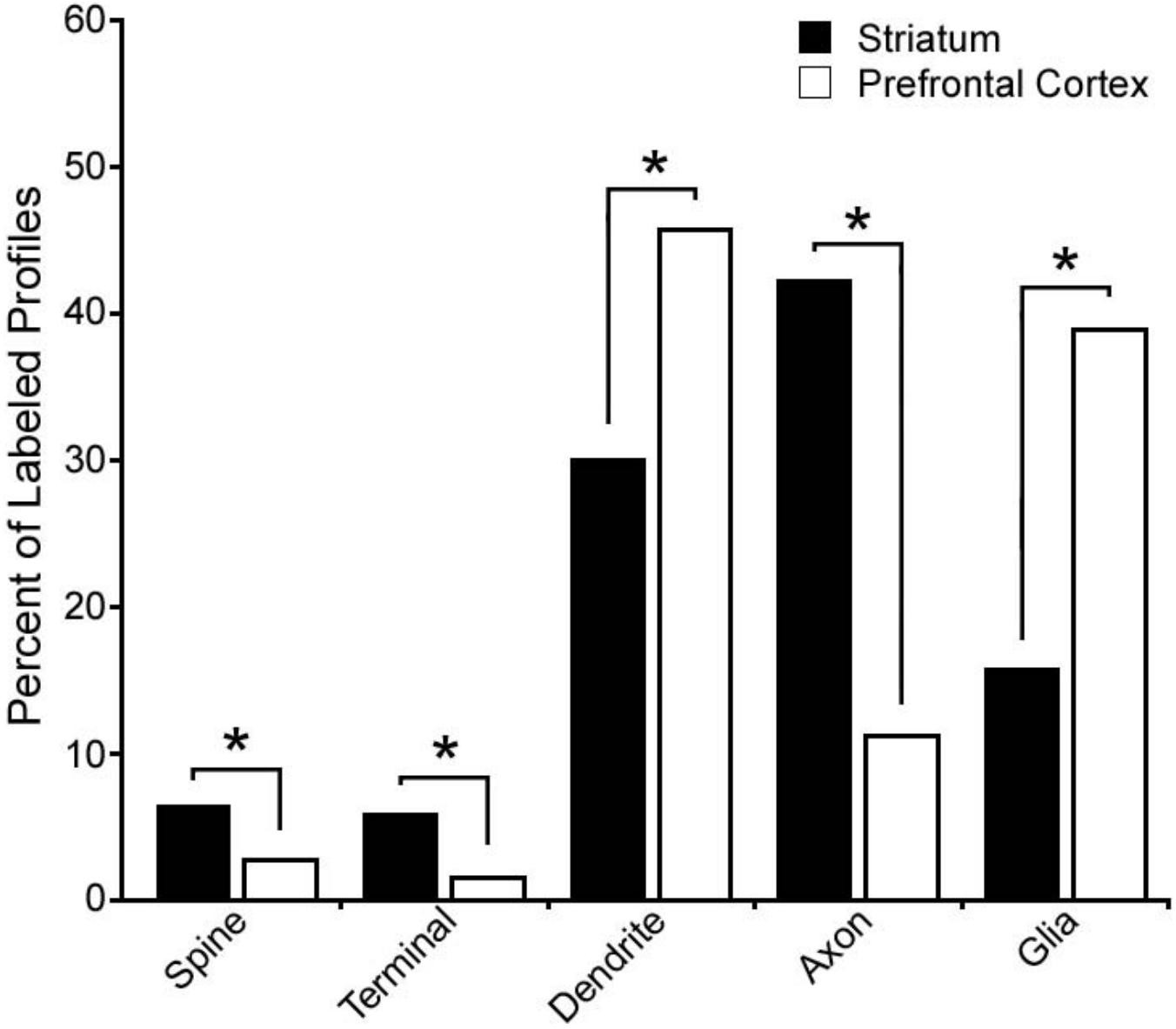

Fig. 9.

Quantitative analysis reveals a selective enrichment of DJ-1 protein in striatal axons, presynaptic terminals, and dendritic spines compared to the cortical DJ-1 distribution. Histograms show the relative distribution of DJ-1-immunreactive elements in the striatum (a total of 615 DJ-1-labeled profiles collected from three monkeys) and in the prefrontal cortex (a total of 584 labeled profiles collected from three monkeys). Chi-square analysis revealed a significant difference between the distribution of DJ-1 in the striatum and prefrontal cortex. Asterisk indicates statistically significant ($p < 0.0001$) difference in the number of DJ-1 immunoreactive profiles in the striatum versus that in the prefrontal cortex.

Table I

Summary of human and monkey tissue used in this study

Sample No.	Age (*yr*)	Sex	PMI[a] (*h*)
Human			
Biochemical analyses			
1	74	Female	3
2	68	Female	11
3	65	Female	6
4	75	Female	6
5	87	Male	20.5
Immunohistochemical analyses			
6	34	Female	22.5
7	51	Male	22.5
8	68	Female	11
9	75	Female	6
10	52	Female	3
Monkey			
Biochemical analyses			
1	3	Male	0
2	1	Male	0
3	1	Female	0
4	1.3	Male	0
Immunohistochemical analyses			
5	2	Male	0
6	2.1	Female	0
7	6.6	Male	0
8	14.8	Female	0

[a] PMI, post-mortem interval.